Eddy Current Testing in the Quantitive Assessment of Degradation State in MAR247 Nickel Superalloy with Aluminide Coatings

Grzegorz Tytko[1] · Małgorzata Adamczyk-Habrajska[2] · Yao Luo[3] · Mateusz Kopec[4]

Abstract

In this paper, the effectiveness of the eddy current methodology for crack detection in MAR 247 nickel-based superalloy with aluminide coatings subjected to cyclic loading was investigated. The specimens were subjected to force-controlled fatigue tests under zero mean level, constant stress amplitude from 300 MPa to 600 MPa and a frequency of 20 Hz. During the fatigue, a particular level of damage was introduced into the material leading to the formation of microcracks. Subsequently, a new design of probe with a pot core was developed to limit magnetic flux leakage and directed it towards the surface under examination. The suitability of the new methodology was further confirmed as the specimens containing defects were successfully identified. The changes in probe resistance values registered for damaged specimens ranged approximately from 8 to 14%.

1 Introduction

The MAR247 nickel superalloy has been extensively utilized in the aerospace industry due to its exceptional mechanical properties, high-temperature resistance, and superior corrosion resistance. This nickel-based alloy has been specifically designed to meet the demanding requirements of modern aircraft engines, where components must withstand extreme temperatures, pressures, and harsh environments while maintaining structural integrity and reliability [1]. The alloy's superior high-temperature performance, combined with its excellent resistance to oxidation and corrosion, make it an ideal material for critical engine components such as turbine blades, vanes, and combustion chambers [2]. However, a key challenge in the application of these alloys is their susceptibility to oxidation and degradation at elevated temperatures, which can significantly deteriorate their performance and limit service life [3]. To address this issue, aluminide coatings have emerged as a promising solution, offering enhanced protection against oxidation and other environmental factors [4]. These coatings form a protective layer of aluminium oxide (Al_2O_3) on the surface, which acts as a barrier against oxygen and other corrosive species. Aluminide coatings have become a widely adopted solution to safeguard gas turbine blades made of superalloys from the detrimental effects of high-temperature oxidation and corrosion [5]. However, the performance and integrity of these coatings are challenged by the complex operating conditions experienced by gas turbines, including cyclic thermal and mechanical loading [4, 5]. The fatigue behavior and cracking of uncoated and coated MAR-M247 superalloy vary significantly between room temperature and

✉ Mateusz Kopec
mkopec@ippt.pan.pl

Grzegorz Tytko
grzegorz.tytko@polsl.pl

Małgorzata Adamczyk-Habrajska
malgorzata.adamczyk-habrajska@us.edu.pl

Yao Luo
luoyao@whu.edu.cn

1   Faculty of Automatic Control, Electronics and Computer Science, Silesian University of Technology, Gliwice 44-100, Poland

2   Faculty of Science and Technology, University of Silesia, Chorzów 41-500, Poland

3   School of Electrical Engineering and Automation, Wuhan University, Wuhan 430072, China

4   Institute of Fundamental Technological Research Polish Academy of Sciences, Pawińskiego 5B, Warsaw 02-106, Poland

elevated temperatures. At room temperature, the uncoated MAR-M247 typically exhibits good fatigue resistance due to its inherent strength and microstructural stability, with fatigue cracks generally initiating at surface defects or inclusions and propagating slowly [6]. When coated, the fatigue life may change depending on the coating material and quality; a well-adhered coating can provide additional protection against surface damage, delaying crack initiation [7, 8]. However, at elevated temperatures, the fatigue resistance of MAR-M247 decreases due to thermal softening and oxidation, which can accelerate crack initiation and growth [9]. Coatings can mitigate these effects by providing a thermal barrier and oxidation protection, thereby enhancing fatigue life. Nonetheless, coating defects or differences in thermal expansion between the coating and substrate may introduce stress concentrations, potentially promoting crack formation under cyclic loading at high temperatures.

The development of advanced material systems for gas turbine applications has been a critical research focus, as designers strive to push the limits of inlet gas temperatures beyond 1300 –1400 °C [5]. The application of coatings on the internal airfoil surfaces has enabled significant improvements in heat removal capabilities, projected to be over 50–70% compared to conventional smooth-channelled, internally cooled airfoil configurations [10]. However, the integrity of these coatings, which are critical to the reliability of gas turbine blades, is challenged by the complex operating conditions experienced during operation. The demanding service environment necessitates the regular inspection of gas turbine blades, enabling a significant reduction in the risk of failures [11]. Non-destructive testing methods can provide valuable insights into the integrity of thermal barrier coatings on nickel-based alloys. These techniques enable for precise detection of defects, corrosion, and other imperfections without causing damage to the materials, which is time-saving and cost-effective [12]. By leveraging non-destructive testing, one can ensure the quality and performance of coated components while maintaining their structural integrity. The multilayer coating-substrate structure and limited access to turbine components expose significant challenges in developing a cost-effective and efficient non-destructive method [13].

In the case of the ultrasonic method [14–16], the most common inconveniences are related to the application of coupling medium, which extends the test time and increases its cost, and the elimination of the dead zone for shallowly located defects. In other methods, the challenge is to ensure sufficient sensitivity, short inspection time, and easy interpretation of results. Therefore, the novelty of this work lies in the development of a new method, that meets all of these requirements enabling effective detection of defects in gas turbine blades. In the first step, the microstructure of coated

MAR 247 nickel-based superalloy subjected to cyclic loading was examined using light microscopy and scanning electron microscopy SEM. This allowed for the determination of the shape, size, and location of damages resulting from intensive exploitation due to fatigue. The shallow depth of critical damages and their relatively large quantity led to the selection of eddy current technique for further investigations. The required sensitivity was achieved by constructing a probe with a pot core diameter corresponding to the blade width at its narrowest point, as it is the most susceptible to crack detection. The application of a pot core enabled the limitation of magnetic flux leakage and directed it towards the surface under examination. Tests were conducted on MAR247 nickel superalloy, onto which coatings of different thicknesses of 20 μm and 40 μm were applied. The damage to the coatings and substrates was induced by subjecting the specimens to fatigue tests at different stress amplitudes. It leads to the formation of damage similar to those during industrial turbine operation. Subsequent eddy current method investigations involved measuring the probe resistance for defect-free specimens and those subjected to fatigue tests. The specimens containing defects were successfully identified in all cases, and the resulting change in probe resistance values ranged approximately from 8 to 14%.

One should highlight, that the novelty of this paper is expressed by the development of a new methodology enabling effective detection of defects in gas turbine blades. This method employs an eddy current probe with the following advantages: the application of a pot core enabled the limitation of magnetic flux leakage and directed it towards the surface under examination (high sensitivity); the outer diameter of the pot-core coil was chosen to be slightly smaller than the width of the inspection area of 15 mm. This reduced the influence of the edge effect on changes in the probe's resistance and facilitated the precise placement of the probe on the examined specimen; the pot-core coil was placed in a head improving the probe's stability; the narrow range of optimal frequency values means that the operating frequency of the probe only needs to be determined once. Therefore, a significant acceleration of the inspection process could be achieved.

2 Materials and Methods

MAR 247 nickel superalloy specimens with three different initial microstructures represented by fine (Fig. 1a), coarse (Fig. 1b) and column (Fig. 1c) grains were manufactured during a conventional casting process. The average grain size these structures was around 0.5 mm, 2.5 mm and 5 mm, respectively. The chemical composition of MAR247
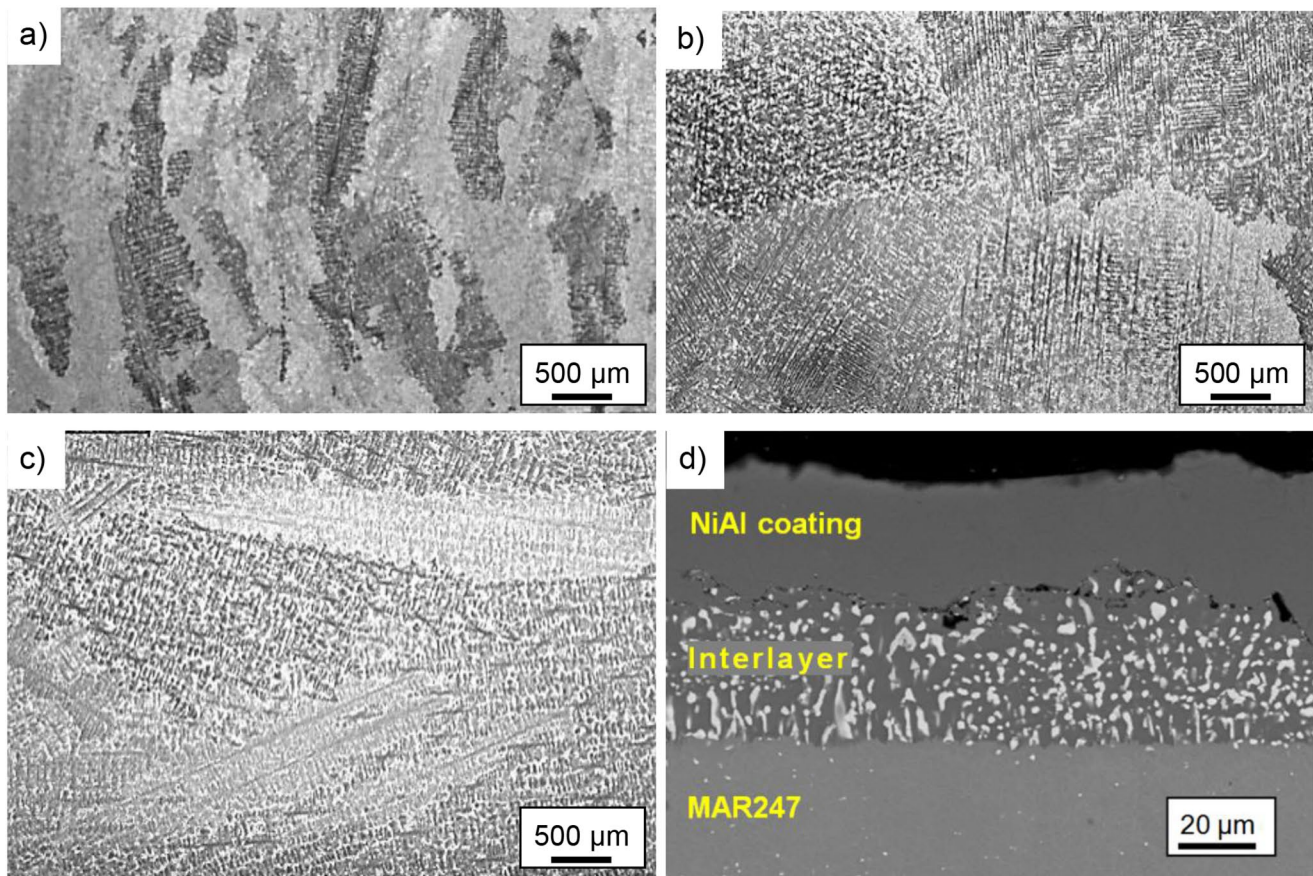
Fig. 1 Initial microstructures of the MAR 247 nickel-based superalloy of fine (**a**), coarse (**b**) and column (**c**) grain structure; cross-section of the MAR 247 specimen with 40 μm coating (**d**)

Table 1 Chemical composition of MAR 247 superalloy (wt%) [17]

C	Cr	Mn	Si	W	Co	Al	Ni
0.09	8.80	0.10	0.25	9.70	9.50	5.70	bal.

nickel superalloy was presented in Table 1. Aluminide coatings were deposited during the Chemical Vapour Deposition (CVD) process. The deposition process was performed at the temperature of 1040 °C and internal pressure of 150 mbar using optimised CVD parameters under the hydrogen protective atmosphere, with deposition times of 8 and 12 h for the coating thickness of 20 μm and 40 μm, respectively. Exemplary cross-section of the MAR 247 specimen with 40 μm coating was presented in Fig. 1d. It reveals a two-layer structure consisting of a homogeneous zone of secondary solid solution of the β (NiAl) phase and heterogeneous NiAl matrix (dark grey) with Ni_3Al phase dispersions (bright grey). The microstructural observations were carried out using a JEOL6360LA scanning electron microscope (SEM) operated at 20 kV with EDS detector.

The MAR 247 nickel superalloy specimens with fine, coarse, and columnar grain structure and coatings of 20 μm and 40 μm thickness [17] were subjected to testing using the eddy current method [18–22]. By inducing electromagnetic currents in the material, eddy current testing can detect surface and subsurface defects, such as cracks, voids, and delaminations, without direct contact. This method is sensitive to variations in coating thickness [23–26], conductivity [27–31], and material properties [32, 33], allowing for detailed and accurate evaluation of the coating's integrity. In the examination of large-scale objects, air-core coil eddy current probes are often used [34–37]. The sensitivity of such a probe is not sufficient for detecting small cracks during inspection of narrow areas. Therefore, a different solution was proposed as follows. The developed probe consists of a coil placed inside a ferrite pot core [38–41]. The application of the core reduced magnetic flux losses and directed it directly towards the surface of the coating. The outer diameter of the pot-core coil, which was equal to 14.5 mm, was chosen to be slightly smaller than the width of the inspection area of 15 mm. This reduced the influence of the edge effect on changes in the probe's resistance and facilitated the precise placement of the probe on the examined

Fig. 2 Pot-core probe and specimens of MAR 247 nickel-based superalloy with 20 μm and 40 μm thick aluminide coatings
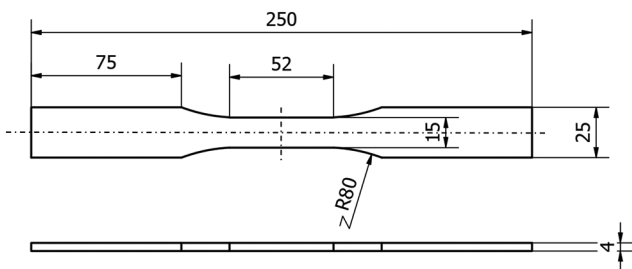

Fig. 3 Engineering drawing of the specimen

specimen. Subsequently, the pot-core coil was placed in a head improving the probe's stability and allowing for the connection of power supply wires (Fig. 2). One should mention, that broad-band excitation was employed to demonstrate how the optimal operating frequency of the probe was selected. Additional aim was to expose, that the sensitivity of the probe is significantly reduced at other frequency values. Once the narrow range of the optimal operating frequency for the probe (165–170 kHz) was established, it was not necessary to utilize broad-band excitation during the conducted tests.

Non-destructive measurements were performed on the specimens' strain gauge length equal to 52 mm as shown in Fig. 3. These specimens were subsequently subjected to cyclic loading using the MTS 810 testing machine. Fatigue tests were force-controlled under zero mean level, constant stress amplitude, frequency of 20 Hz and stress amplitude ranging from 300 MPa to 600 MPa. Such fatigue testing was performed at room temperature to introduce a specific level of damage similar to those during industrial turbine operation. In this research, the $0.5N_f$ was used as a reference point to interrupt fatigue tests in order to perform EC measurements. Subsequently, the presence of cracks due to cyclic loading was confirmed by using JEOL6360LA scanning electron microscope observations. Each specimen was characterized by a notable number of cracks with a depth of <0.5 mm. The exemplary view of formed cracks was presented in Fig. 4 for the specimen with 20 μm (a) and 40 μm (b) thick coating.

3 Results

The resistance measurements of the eddy current probe were carried out using the Keysight E4980A precision LCR meter with an accuracy of +/− 0.05%, in the frequency range from 130 kHz to 280 kHz. Eight measurements were performed for each frequency value, from which the arithmetic mean was calculated. At the beginning of the experiment, the reference resistance values R_{REF} were measured for specimens without defects. In the second step, the resistance R of the probe placed on specimens subjected to fatigue tests under stress amplitudes from 300 MPa to 600 MPa was measured. The probe was moved along the symmetry axis of the sample with a step of 2 mm, and the final measurement point was the one where the largest changes in resistance value compared to R_{REF} were obtained. The relative resistance difference δR expressed in [%] was defined according to (1) for
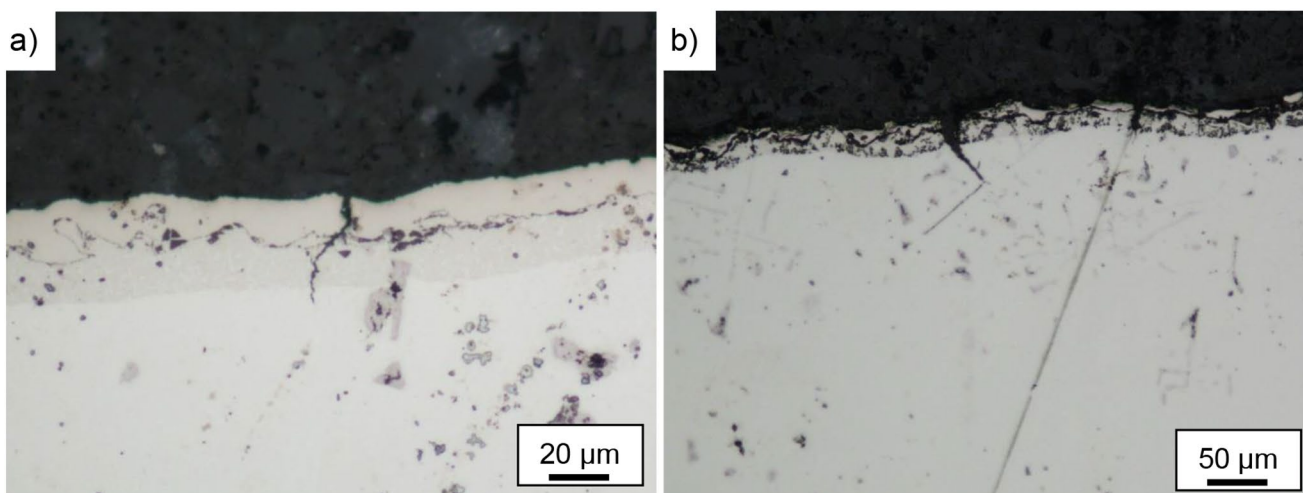

Fig. 4 Different types of cracks formed during fatigue testing in the specimen with 20 μm (**a**) and 40 μm (**b**) thick coating

comparison purposes. The highest value of δR obtained for the specimen in the entire frequency range from 130 kHz to 280 kHz was marked as δR_{MAX} (Fig. 5).

$$\delta R = \frac{R_{REF} - R}{R_{REF}} \cdot 100\% \tag{1}$$

The resistance difference values δR obtained for specimens with 20 μm coating were presented for column (Fig. 6a), fine (Fig. 6b), and coarse (Fig. 6c) grain structures. In Fig. 6d, the resistance differences were shown for these three-grain structures when subjected to the stress amplitude of 500 MPa. The highest resistance change values determined by the parameter δR_{MAX}, obtained for these specimens, are shown in Fig. 5a. Subsequently, the measurement results for specimens with 40 μm coatings were presented (Fig. 6e), and the column, fine, and coarse structures were compared for a stress amplitude of 500 MPa (Fig. 6f). The values of the parameter δR_{MAX} are shown in Fig. 5.

4 Discussion

In all measurements conducted using the eddy current method, the resistance value of the probe significantly changed after subjecting the specimens to cyclic loading. The obtained values of the δR coefficient confirmed and ensured a clear distinction between reference specimens and those containing structural damage due to fatigue. Achieving such good results requires the careful selection of the proper inspection parameters. It was found, that the required

sensitivity of the probe can be achieved by using a pot core. Limiting the leakage of magnetic flux enables satisfactory changes in the resistance of the probe to be obtained. Additionally, the reactance value of the probe could be also measured, but changes of around 3% proved insufficient to infer the presence of defects in the specimens. Applying a probe with a diameter close to the width of the examined area had two main advantages. Firstly, it reduced the edge effect compared to a probe with a larger diameter. The second advantage was facilitating the precise placement of the probe relative to the surface being examined so that all measurement points were located on the sample's axis of symmetry.

Preliminary measurements conducted in the frequency range from 1 kHz to 1 MHz enabled the determination of the optimal operating frequency value. For low frequencies, the δR parameter value is relatively small. A significant change occurs near the resonant frequency of about 130 kHz. Above the resonant frequency, there is a sharp increase in the value of δR, followed by its steady decrease. For such a reason, the frequency range from 130 kHz to 280 kHz was used for further research. The δR coefficient was assumed as the highest value for frequencies of 165–170 kHz. Such a narrow range of optimal frequency values means that the operating frequency of the probe only needs to be determined once. Therefore, a significant acceleration of the inspection process could be achieved.

The frequency at which the δR coefficient reaches its maximum value also provides information about the location of damage in the specimen structure. The standard penetration depth for a frequency $f = 170$ kHz is 0.28 mm,
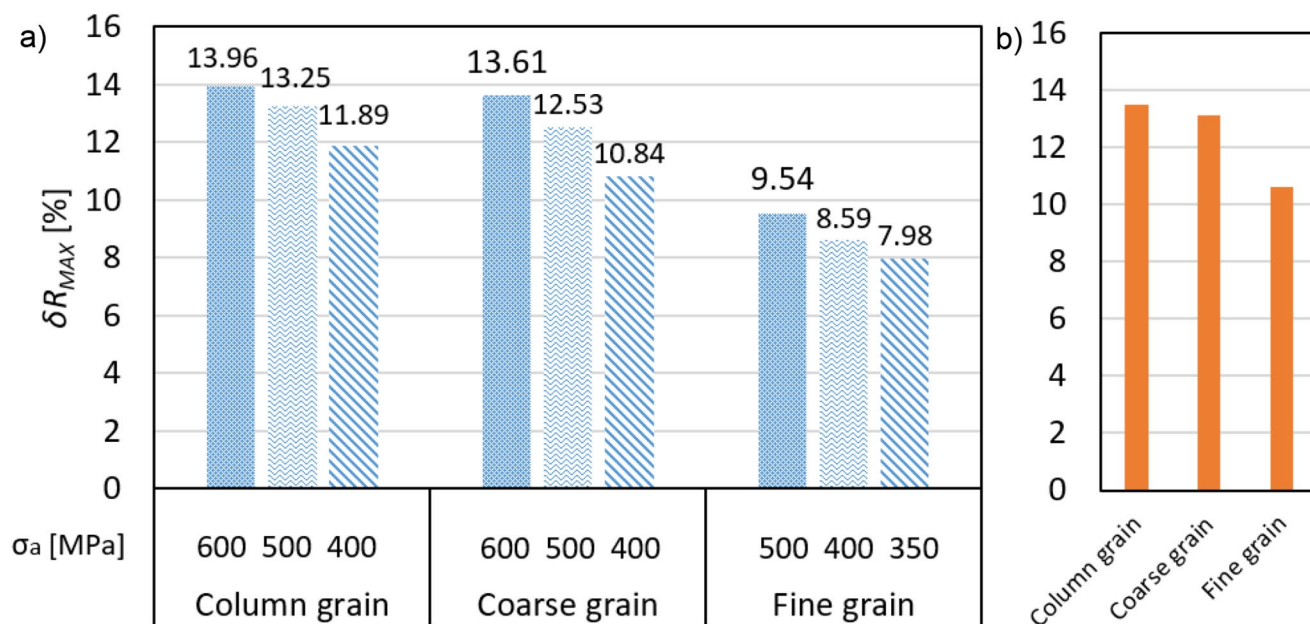

Fig. 5 Maximum values of resistance measured for specimens with 20 μm (**a**) and 40 μm thick coatings when subjected to stress amplitude equal to 500 MPa (**b**)
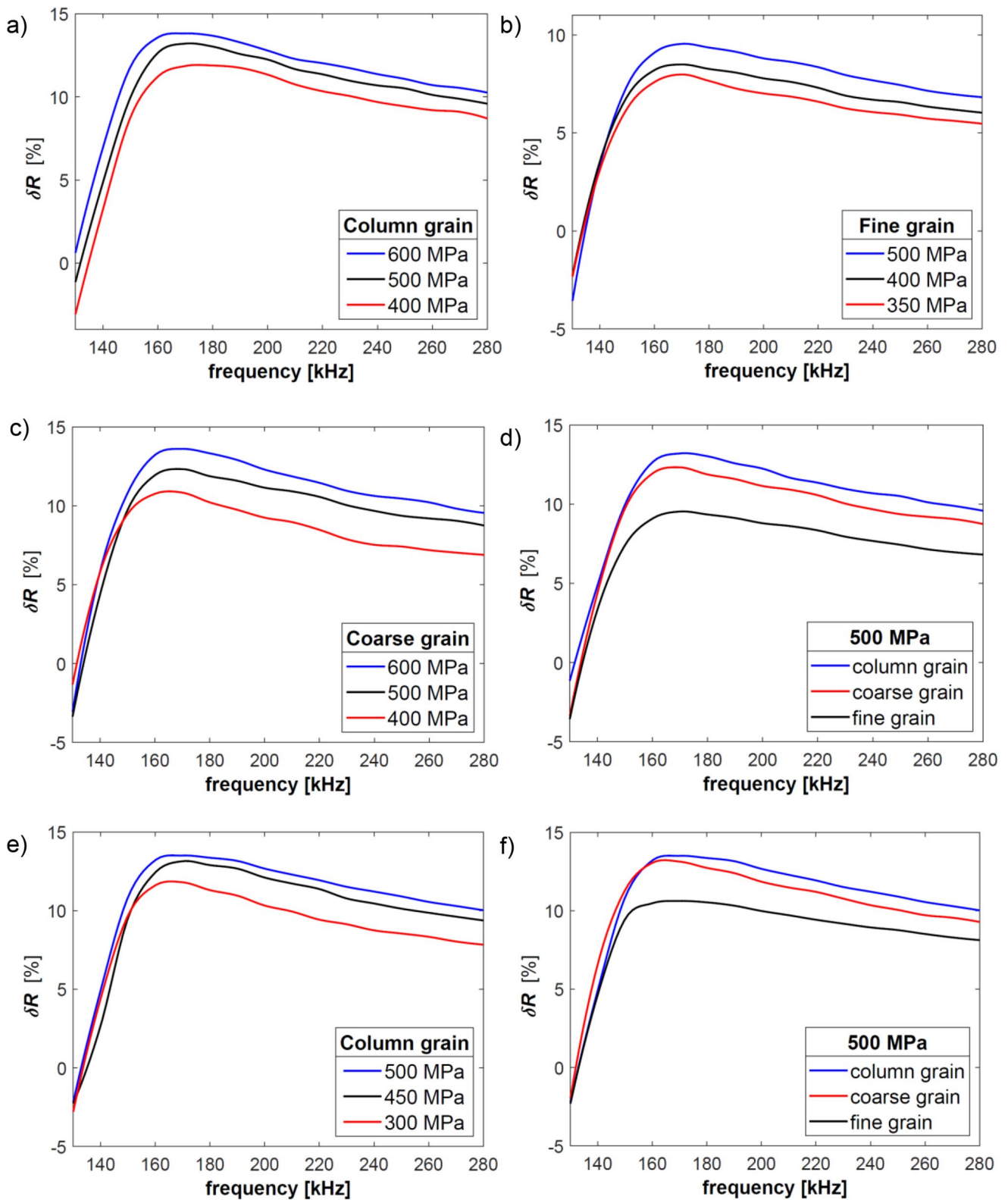
Fig. 6 Resistance changes δR registered for specimens with: column grain structure and coating thickness equal to 20 μm (**a**); fine grain structure and coating thickness equal to 20 μm (**b**) coarse grain structure and coating thickness equal to 20 μm (**c**); coating thickness equal to 20 μm subjected to fatigue testing at stress amplitude of 500 MPa (**d**); column grain structure and coating thickness equal to 40 μm (**e**) coating thickness equal to 40 μm subjected to fatigue testing at stress amplitude of 500 MPa (**f**)

indicating that structural damage is primarily located shallow beneath the specimen surface. Based on the obtained reference resistance values R_{REF} (for $f = 130$–280 kHz), there is no possibility to distinguish specimens under investigation. A difference in coating thickness of 20 μm is too small to have a significant impact on the probe resistance value. Furthermore, the type of initial microstructure (fine, coarse, or column) does not significantly alter the flow of eddy currents.

The results of the measurements presented in Fig. 6 confirmed that the increase in stress amplitude has a significant influence on changes in probe resistance caused by the occurrence of damage. This influence is more significant for lower amplitude values (300–400 MPa) than for higher ones (500–600 MPa). In all cases, the smallest resistance changes were obtained for fine grain samples. These values significantly differed from those obtained for the other initial microstructures. The differences in δR values shown in Figs. 4 and 5 are caused by the formation of different crack and micropore configurations in samples with different initial microstructures, using the same stress amplitude. Each such crack disrupts the flow of eddy currents, causing a change in the probe resistance value.

Non-destructive methods for detecting cracks in materials with thermal barrier coatings (TBCs) are essential for ensuring the reliability and longevity of components, particularly in high-temperature applications like gas turbines and aero engines. Among these methods, infrared thermography is highly effective, leveraging thermal imaging to detect surface and subsurface cracks by observing thermal contrasts caused by differences in heat flow through the material [42]. Another advanced technique is ultrasonic testing, which uses high-frequency sound waves to detect flaws; in TBCs, this method is particularly useful for identifying delaminations and vertical cracks that may not be visible on the surface [43]. Additionally, laser shearography, an optical method, is effective in identifying surface and near-surface defects by detecting the deformation response of a material under stress [44]. X-ray computed tomography (CT) scanning offers detailed internal imaging, capable of detecting fine cracks and porosity within the coating and substrate, providing a comprehensive view of material integrity [45]. Each of these methods has its strengths and limitations, often dictated by the specific characteristics of the TBC, the type of substrate material, and the nature of the cracks; thus, a combination of techniques is often employed to achieve the most accurate assessment of crack presence and propagation in materials with thermal barrier coatings. In comparison to these methods, the eddy current method is superior in its sensitivity to small cracks and its ability to provide rapid and localized assessments, which makes it particularly effective for early-stage detection and in situations where surface access is limited or the inspection area is complex [46]. Additionally, ECT can be highly automated and easily integrated into maintenance routines, providing real-time data and reducing inspection times. However, the method is deficient when dealing with materials that have thick TBCs, as the coating can attenuate the eddy currents, reducing the method's sensitivity to subsurface defects. Moreover, ECT is limited in detecting cracks that are oriented parallel to the surface or those located deeper below the coating, where the electromagnetic fields are less effective. In such cases, other non-destructive testing methods, such as ultrasonic testing or thermography, may be more suitable, as they can penetrate thicker coatings and detect deeper or differently oriented cracks. Overall, while eddy current testing is a valuable tool for detecting cracks in materials with thermal barrier coatings, its effectiveness can be compromised by the thickness of the coating and the orientation and depth of the defects, necessitating the use of complementary inspection techniques for comprehensive evaluation.

One should mention, the literature on EC crack detection in gas turbine blades made of nickel alloys. Furthermore, it is difficult to compare the results, which require interpretation of the obtained scans, with the numerical data obtained in the developed methodology presented in this work. Therefore, some examples of eddy current application in the assessment of coatings under fatigue or prolonged service were discussed. Uchanin [47] presented low-frequency double differential eddy current probes with enhanced capability for detecting subsurface cracks were introduced. These probes come in various sizes, from 5 to 33 mm, and offer different spatial resolutions for specific applications. They operate across a wide frequency range, from 0.2 kHz to 1.0 MHz, with high penetration depth and exceptional sensitivity to subsurface defects. The probes are particularly effective in detecting fatigue cracks in multilayer structures, such as riveted aircraft components and repaired surfaces. This technology enables timely detection of dangerous damage without needing to disassemble aircraft or remove protective coatings. Grosso et al. [48] performed conventional eddy current testing (ECT) on samples consisting of carbon steel substrates coated with anticorrosive composites commonly used inside petrochemical storage tanks. Simulated localized corrosion, represented by undercoating defects, was detected by inspecting the same side as the machined defects. With defect diameters in the millimeter range, the results suggest that ECT is capable of identifying corrosion in its early stages. The accuracy of the method was unaffected by coating thicknesses ranging from approximately 300 to 1000 μm, as well as the presence of corrosion products. Additionally, multilevel threshold processing enhanced defect detectability by eliminating false positives, which typically arise from thickness variations

inherent to the coating application process. Savari et al. [49] presented eddy-current testing of fatigue degradation under contact loading of NiCrBSi coatings obtained through gas–powder laser cladding. The EC method has proven effective for testing fatigue degradation in NiCrBSi coatings subjected to contact loading, with coatings produced via gas-powder laser cladding and containing various levels of chromium, boron, carbon, and 15–25 wt% TiC additives. High excitation frequencies, particularly 120 kHz, provide optimal results by minimizing the influence of the ferromagnetic steel base and analyzing the thinnest surface layer where cracking and compaction occur. Testing TiC–PG-SR2 composite coatings with 15 wt% TiC is limited to early stages (up to 10^5 cycles) due to the presence of discontinuities, and should be conducted at maximum excitation frequencies to detect surface-level fatigue. For coatings with 25 wt% TiC, the fatigue degradation process is better tracked at lower frequencies (36 kHz), where cracking has less impact on EC readings. The discontinuities in the composite coatings accelerate both cracking and compaction, which have opposing effects on resistivity. Therefore, the EC method offers reliable testing for different TiC compositions, but must be adjusted based on the coating's TiC content and the stage of degradation. Gonchar et al. [50] showed the eddy-current and ultrasonic investigations of the nickel-base superalloy the gas turbine engine blades after exploitation. The study found that gas turbine engine blades made from nickel-based superalloys experience significant changes in electromagnetic and acoustic properties, in addition to softening, when subjected to operational overheating. The phase shift of the eddy-current probe increased by more than twofold, the velocity of longitudinal ultrasonic waves decreased by 200 m/s, and attenuation was halved. Optimal testing of the superalloy's electromagnetic properties occurred at 100 kHz, providing stable readings and maximum sensitivity. These findings suggest a potential method for operational control of turbine blade material through non-destructive testing. Das et al. [51] reported frequency scanning eddy current testing (F-SECT) for condition assessment of multiple layers of coating on gas turbine blades. It was proven, that such technique can be used to evaluate the condition of MCrAlY coatings on gas turbine blades and vanes. It serves as a quality control tool for inspecting both new and refurbished blades, as well as optimizing refurbishment intervals. This method is particularly relevant for gas turbine units operating under partial loading, where refurbishment may not be required based solely on operating hours. FSECT is anticipated to reduce unnecessary maintenance and lower the life cycle costs of coated blades and vanes.

5 Conclusion

The conducted research using the eddy current method has demonstrated its effectiveness in detecting structural damage due to fatigue by measuring changes in probe resistance. Significant differences in the δR coefficient distinguished damaged specimens from references, demonstrating the method's sensitivity. Optimal measurement accuracy was achieved by using a pot core, selecting appropriate probe diameters, and operating at frequencies around 165–170 kHz, where the δR coefficient was highest. The sensitivity was more noticeable at lower stress amplitudes and varied with initial microstructures, although fine grain samples showed minimal resistance changes. The study highlights the importance of optimizing inspection parameters to improve the reliability of the eddy current method in detecting material damage.

Author Contributions G. T.: Conceptualization, Data curation, Formal analysis, Investigation, Methodology, Project administration, Supervision, Validation, Visualization, Roles/Writing - original draft, Writing - review & editing. M. A.-H.: Data curation, Investigation, Validation. Y. L.: Formal analysis, Methodology. M. K.: Conceptualization, Data curation, Formal analysis, Investigation, Methodology, Project administration, Supervision, Validation, Visualization, Roles/Writing - original draft, Writing - review & editing.

Data Availability No datasets were generated or analysed during the current study.

Declarations

References

1. Ramsperger, M., Eichler, S.: Electron Beam Based Additive Manufacturing of Alloy 247 for turbine engine application: From Research towards Industrialization. Metall. Mater. Trans. A. **54**, 1730 (2023). https://doi.org/10.1007/s11661-022-06955-0

2. Jordan, O., Lion, P., Beck, T.: Short-time creep deformation of the coarse-grained nickel-base alloy 247 and its implications on the high-cycle fatigue behavior. ASME J. Eng. Gas Turbines Power. **145**(5), 051015 (2023). https://doi.org/10.1115/1.4056309

3. Li, D.S., Chen, G., Li, D., et al.: Oxidation resistance of nickel-based superalloy inconel 600 in air at different temperatures. Rare Met. **40**, 3235 (2021). https://doi.org/10.1007/s12598-018-1148-1

4. Kopec, M.: Recent advances in the deposition of Aluminide Coatings on Nickel-based superalloys: A synthetic review (2019–2023). Coatings. **14**(5), 630 (2024). https://doi.org/10.3390/coatings14050630

5. Barwinska, I., Kopec, M., Kukla, D., et al.: Thermal barrier Coatings for High-Temperature performance of Nickel-based superalloys: A synthetic review. Coatings. **13**(4), 769 (2023). https://doi.org/10.3390/coatings13040769

6. Šulák, I., Obrtlík, K., AFM: SEM AND TEM study of damage mechanisms in cyclically strained mar-M247 at room temperature and high temperatures. Theoret. Appl. Fract. Mech. **108**, 102606 (2020). https://doi.org/10.1016/j.tafmec.2020.102606

7. Šulák, I., Obrtlík, K., Čelko, L., Gejdoš, P., Jech, D.: High-temperature low-cycle fatigue behaviour of MAR-M247 coated with newly developed thermal and environmental barrier coating. Adv. Mater. Sci. Eng. 9014975 (2018). https://doi.org/10.1155/2018/9014975

8. Kopec, M.: Effect of Aluminide Coating thickness on high-temperature fatigue response of MAR-M247 nickel-based Superalloy. Coatings. **14**, 1072 (2024). https://doi.org/10.3390/coatings14081072

9. Šulák, I., Obrtlík, K.: Thermomechanical and isothermal fatigue properties of MAR-M247 superalloy. Theoret. Appl. Fract. Mech. **131**, 104443 (2024). https://doi.org/10.1016/j.tafmec.2024.104443

10. Alvin, M.A., Klotz, K., McMordie, B., et al.: Extreme Temperature Coatings for Future gas turbine engines. ASME. J. Eng. Gas Turbines Power. **136**(11), 112102 (2014). https://doi.org/10.1115/1.4027186

11. Rajendran, R., Ganeshachar, M.D., Jivankumar, T., et al.: Condition assessment of gas turbine blades and coatings. Eng. Fail. Anal. **18**(8), 2104 (2011). https://doi.org/10.1016/j.engfailanal.2011.06.017

12. Vasagar, V., Hassan, M.K., Abdullah, A.M., et al.: Non-destructive techniques for corrosion detection: A review. Corros. Eng., Sci. Technol. **59**(1), 56 (2024). https://doi.org/10.1177/1478422X241229621

13. Balasubramanian, V., Niksan, O., Jain, M.C., et al.: Non-destructive erosive wear monitoring of multi-layer coatings using AI-enabled differential split ring resonator based system. Nat. Commun. **14**, 4916 (2023). https://doi.org/10.1038/s41467-023-40636-9

14. Luo, K., Zhu, J., Li, Z., et al.: Ultrasonic Lamb Wave damage detection of CFRP composites using the bayesian neural network. J. Nondestruct Eval. **43**, 48 (2024). https://doi.org/10.1007/s10921-024-01054-z

15. Luo, Z., Liu, Z., Li, F., et al.: Defects imaging in Corner Part with Surface Adaptive Ultrasonic and focusing in receiving (FiR) strategy. J. Nondestruct Eval. **43**, 49 (2024). https://doi.org/10.1007/s10921-024-01063-y

16. Mohd Tahir, M.F., Echtermeyer, A.T.: Phased array Ultrasonic Testing on Thick Glass Fiber Reinforced Thermoplastic Composite Pipe implementing the classical time-corrected Gain Method. J. Nondestruct Eval. **43**, 74 (2024). https://doi.org/10.1007/s10921-024-01096-3

17. Kukla, D., Kopec, M., Kowalewski, Z.L., Politis, D.J., Jóźwiak, S., Senderowski, C.: Thermal Barrier Stability and wear behavior of CVD deposited Aluminide Coatings for MAR 247 Nickel Superalloy. Materials. **13**(17), 3863 (2020). https://doi.org/10.3390/ma13173863

18. Du, Y., Zhang, Z., Yin, W.: Et. Al. Sloping-invariance for nonferrous metallic slabs at multiple frequencies by eddy current sensors. IEEE Access. **9**, 59949–59956 (2021)

19. Yu, D., Chen, B., Luo, Y., et al.: Mutual inductance calculation for rectangular and circular coils with parallel axes. IET Electr. Power Appl. **18**(4), 379 (2023). https://doi.org/10.1049/elp2.12396

20. Tytko, G.: Eddy current testing of conductive coatings using a pot-core sensor. Sensors. **23**(2), 1042 (2023)

21. Poletkin, K., Babic, S.: Calculation of magnetic stiness over Torque between two current-carrying circular filaments arbitrarily positioning in the space. J. Magn. Magn. Mater. **603**, 172202 (2024). https://doi.org/10.1016/j.jmmm.2024.172202

22. Cui, L., Zeng, Z., Jiao, S.: Finite Element Analysis of Eddy Current Testing of Aluminum Honeycomb Sandwich Structure with CFRP panels based on the Domain Decomposition Method. J. Nondestruct Eval. **43**, 44 (2024). https://doi.org/10.1007/s10921-024-01053-0

23. Zhang, D., Yu, Y., Lai, C., et al.: Thickness measurement of multi-layer conductive coatings using multifrequency eddy current techniques. Nondestructive Test. Evaluation. **31**(3), 191 (2016). https://doi.org/10.1080/10589759.2015.1081903

24. Li, Y., Wang, Y., Liu, Z., et al.: Characteristics regarding lift-off intersection of pulse-modulation Eddy current signals for evaluation of hidden thickness loss in Cladded conductors. Sensors. **19**, 4102 (2019). https://doi.org/10.3390/s19194102

25. Wang, Z., Yu, Y.: Thickness and conductivity measurement of multilayered electricity-conducting coating by pulsed Eddy current technique: Experimental investigation. IEEE Trans. Instrum. Meas. **68**(9) (2019). https://doi.org/10.1109/TIM.2018.2872386

26. Meng, X., Lu, M., Yin, W., et al.: Evaluation of Coating Thickness using lift-off insensitivity of Eddy Current Sensor. Sensors. **21**, 419 (2021). https://doi.org/10.3390/s21020419

27. Yu, Y., Zhang, D., Lai, C., et al.: Quantitative Approach for thickness and conductivity measurement of monolayer coating by dual-frequency Eddy current technique. IEEE Trans. Instrum. Meas. **66**(7), 1874 (2017). https://doi.org/10.1109/TIM.2017.2669843

28. Liu, Y., Zhang, Z., Yin, W.: A novel conductivity classification technique for Nonmagnetic Metal Immune to Tilt variations using Eddy current testing. IEEE Access. **9**, 135334 (2021). https://doi.org/10.1109/ACCESS.2021.3116247

29. Xu, J., Wu, J., Xin, W., et al.: Fast measurement of the Coating Thickness and Conductivity using Eddy currents and Plane Wave Approximation. IEEE Sens. J. **21**(1) (2021). https://doi.org/10.1109/JSEN.2020.3014677

30. Huang, P., Li, Z., Pu, H., et al.: Conductivity Measurement of non-magnetic material using the phase feature of Eddy Current Testing. J. Nondestruct Eval. **42**, 50 (2023)

31. Cao, B., Sun, J., Fan, M., et al.: Novel conductivity measurement of thin metallic materials using crossover frequency feature from triple-frequency Eddy current signals. IEEE Trans. Instrum. Meas. **73**, 6005611 (2024). https://doi.org/10.1109/TIM.2024.3383059

32. Xu, J., Wu, J., Xin, W., et al.: Measuring ultrathin metallic Coating properties using swept-frequency Eddy-current technique. IEEE Trans. Instrum. Meas. **69**(8) (2020). https://doi.org/10.1109/TIM.2020.2966359

33. Li, Y., Chen, Z., Mao, Y., et al.: Quantitative evaluation of thermal barrier coating based on eddy current technique. NDT&E Int. **50**, 29 (2012). https://doi.org/10.1016/j.ndteint.2012.04.006

34. Tytko, G.: Locating defects in conductive materials using the Eddy Current Model of the Filamentary Coil. J. Nondestruct Eval. **40**, 66 (2021). https://doi.org/10.1007/s10921-021-00798-2

35. Yang, X., Luo, Y., Kyrgiazoglou, A.: Et. Al. Impedance variation of a reflection probe near the edge of a magnetic metal plate. IEEE Sens. J. **23**(14), 15479–15488 (2023)

36. Li, C., Guo, Z., Zhen, M., et al.: A non-contact rotational speed sensor for bearing cages in a high-temperature and high-speed environment. IEEE Sens. J. (2024). https://doi.org/10.1109/JSEN.2024.3405793

37. Deng, Z., Wang, Y., Shi, Q., et al.: 2-D Analytical Model of Sinusoidal Eddy Current Field based on permeability distortion. IEEE Sens. J. 24(9), 14392 (2024). https://doi.org/10.1109/JSEN.2024.3376804

38. Tytko, G.: An eddy current model of pot-cored coil for testing multilayer conductors with a hole. Bull. Pol. Acad. Sci. Tech. Sci. 68(6), 1311 (2020). https://doi.org/10.24425/bpasts.2020.135388

39. Zhang, S.: Analytical Model of an E-core driver-pickup coils Probe Applied to Eddy Current Testing of Multilayer Conductor. ACES J. 38(11), 914 (2023). https://doi.org/10.13052/2023.ACES.J.381110

40. Praphaphankul, N., Akutsu, A., Sasaki, E.: Numerical study for development of subsurface crack detection using pulsed eddy current and swept frequency eddy current. Struct. Infrastruct. Eng. 1 (2023). https://doi.org/10.1080/15732479.2023.2218351

41. Tytko, G., Dziczkowski, L., Magnuski, M., et al.: Eddy current testing of conductive discs using the pot-core sensor. Sens. Actuators A: Phys. 349, 114060 (2023)

42. Zhu, J., Mao, Z., Wu, D., et al.: Progress and trends in nondestructive testing for Thermal Barrier Coatings based on Infrared Thermography: A review. J. Nondestruct Eval. 41(49) (2022). https://doi.org/10.1007/s10921-022-00880-3

43. Bychenok, V.A., Khizhnyak, S.A., Sorokin, A.A., et al.: Ultrasonic Testing of Adhesion of Special Coatings. Russ J. Nondestruct Test. 59, 839–846 (2023). https://doi.org/10.1134/S1061830923700481

44. Siang, T.W., Firdaus Akbar, M., Nihad Jawad, G.: A past, Present, and prospective review on microwave nondestructive evaluation of Composite Coatings. Coatings. 11, 913 (2021). https://doi.org/10.3390/coatings11080913

45. Błachnio, J., Chalimoniuk, M., Kułaszka, A.: Et. Al. Exemplification of detecting gas turbine blade structure defects using the X-ray computed Tomography Method. Aerospace. 8, 119 (2021). https://doi.org/10.3390/aerospace8040119

46. AbdAlla, A.N., Faraj, M.A., Samsuri, F.: Et. Al. Challenges in improving the performance of eddy current testing. Rev. Meas. Control. 52(1–2), 46–64 (2019). https://doi.org/10.1177/0020294018801382

47. Uchanin, V.: Eddy current techniques for detecting hidden subsurface defects in Multilayer Aircraft structures. Trans. Aerosp. Res. 2, 69–79 (2022). https://doi.org/10.2478/tar-2022-0011

48. Grosso, M., Pacheco, C.J., Arenas, M.P.: Et. Al. Eddy current and inspection of coatings for storage tanks. J. Mater. Res. Technol. 7(3), 356–360 (2018). https://doi.org/10.1016/j.jmrt.2018.05.006

49. Savrai, R.A., Makarov, A.V., Gorkunov, E.S.: Eddy-current testing of fatigue degradation under contact loading of NiCrBSi coatings obtained through gas–powder laser cladding. Russ J. Nondestruct Test. 51, 692–704 (2015). https://doi.org/10.1134/S1061830915110042

50. Gonchar, A.V., Mishakin, V.V., Klushnikov, V.A., Kurashkin, K.V.: The eddy-current and ultrasonic investigations of the nickel-base superalloy the gas turbine engine blades after exploitation. J. Phys.:Conf. Ser. 2131, 052025 (2021). https://doi.org/10.1088/1742-6596/2131/5/052025

51. Das, A., Chhabra, A., Mondal, A., et al.: Frequency Scanning Eddy Current testing (F-SECT) for condition assessment of multiple layers of Coating on Gas Turbine Blades. Indian National Seminar & Exhibition on Non-Destructive Evaluation NDE 2015, Hyderabad, India. Journal of Nondestructive Testing, 22(6) (2017)